GEOPHYSICAL RESEARCH LETTERS, VOL. 25, NO.10, PAGES 1705-1708, MAY 15, 1998

Sources and chemistry of NO_x in the upper troposphere over the United States

L. Jaeglé,[1] D. J. Jacob,[1] Y. Wang,[1] A. J. Weinheimer,[2] B. A. Ridley,[2] T. L. Campos,[2] G. W. Sachse,[3] D. E. Hagen[4]

Abstract. The origin of NO_x in the upper troposphere over the central United States is examined using aircraft observations obtained during the SUCCESS campaign in April-May of 1996. Correlations between NO_y (sum of NO_x and its oxidation products) and CO at 8-12 km altitude indicate that NO_x originates primarily from convective transport of polluted boundary layer air. Lightning and aircraft emissions appear to be only minor sources of NO_x. Chemical steady state model calculations constrained by local observations of NO underestimate the measured NO_x/NO_y concentration ratio at 8-12 km altitude by a factor of two on average. The magnitude of the underestimate is correlated with concentrations of condensation nuclei, which we take as a proxy for the age of air in the upper troposphere. We conclude that the NO_x/NO_y ratio is maintained above chemical steady state by frequent convective injections of fresh NO_x from the polluted boundary layer and by the long lifetime of NO_x in the upper troposphere (5-10 days). In contrast to previous studies, we find no evidence for fast heterogeneous recycling from HNO_3 to NO_x in the upper troposphere.

Introduction

Human influence on ozone concentrations in the upper troposphere is receiving increased attention because of its potential contribution to climate change. Ozone is an effective greenhouse gas in the upper troposphere [*Fishman et al.*, 1979; *Lacis et al.*, 1990]. In that region, the production of ozone is catalyzed by nitrogen oxides (NO_x=NO+NO_2) which may originate from lightning, downwelling of stratospheric air, aircraft emissions, and surface emissions (including from fossil fuel combustion) transported convectively to the upper troposphere [*Brasseur et al.*, 1996]. Much of the uncertainty regarding the extent of human influence on ozone in the upper troposphere revolves around the anthropogenic contribution to NO_x levels in that region.

Understanding the origin of NO_x in the upper troposphere is complicated by the chemical cycling of NO_x with its oxidation products including nitric acid (HNO_3), pernitric acid (HNO_4), and peroxyacetyl nitrate (PAN). At equilibrium only a small fraction of total NO_y (sum of NO_x and its oxidation products) may be present as NO_x. Recent studies of the remote troposphere have indicated that the cycling between NO_x and its principal reservoir, HNO_3, is poorly understood: photochemical models systematically underestimate observations of the NO_x/HNO_3 concentration ratio [*Liu et al.*, 1992; *Fan et al.*, 1994; *Jacob et al.*, 1996]. Possible heterogeneous mechanisms have been proposed to reconcile models and observations [*Chatfield*, 1994; *Fan et al.*, 1994; *Jacob et al.*, 1996; *Hauglustaine et al.*, 1996].

[1]Harvard University, Cambridge, Massachusetts.
[2]NCAR, Boulder, Colorado.
[3]NASA Langley Research Center, Hampton, Virginia.
[4]University of Missouri, Rolla, Missouri.

Paper number 97GL03591.
0094-8534/98/97GL-03591$05.00

In this paper we examine the factors controlling NO_x concentrations in the upper troposphere over the United States, by interpreting recent observations obtained during the SUCCESS (SUbsonic aircraft: Cloud and Contrail Effects Special Study) aircraft mission. In a first step we examine the primary origin of NO_y in the upper troposphere using tracer correlations. In a second step, we test our understanding of the chemical cycling of NO_x using the observed NO_x/NO_y concentration ratios. A companion paper [*Jaeglé et al.*, this issue] combines the NO_x and HO_x (=OH+peroxy radicals) observations in SUCCESS to calculate ozone production in the upper troposphere and determine its sensitivity to NO_x.

Observations and Model

The SUCCESS mission [*Toon et al.*, this issue] took place in April-May of 1996 out of Salina, Kansas (Figure 1). Simultaneous measurements of NO, NO_y, N_2O, O_3, OH, HO_2, H_2O, CO, CO_2 and CH_4 concentrations were made up to 12.5 km altitude together with aerosol, cloud, and radiative observations.

Most flights during SUCCESS were designed to sample clouds, contrails, and aircraft exhaust. Yet, many measurements were made in cloud-free and exhaust-free environments and, in this study, we will focus on understanding these background observations. We selected the data according to aerosol surface area (< 20 $\mu m^2/cm^3$) to eliminate observations made in clouds. Fresh aircraft exhaust plumes were diagnosed and excluded on the basis of enhancements in both CO_2 (> 368 ppmv) and NO (> 300 pptv). All flights examined here were conducted during daytime.

Concentrations of O_3, NO and NO_y were measured by chemiluminescence [*Ridley et al.*, 1994]. NO_y was sampled through an inlet perpendicular to the direction of air flow, discriminating against particulate NO_y, and thus allowing the measurement of gas phase NO_y only. Aerosol nitrate amounted to 5-15% of gas phase NO_y in cloud-free air [*Talbot et al.*, this issue]. A common interferer to the NO_y concentration measurement is HCN [*Kliner et al.*, 1997]. In-flight measurements of the HCN conversion efficiency to NO_y were in the range of 1.2-7.5%. Assuming a mean

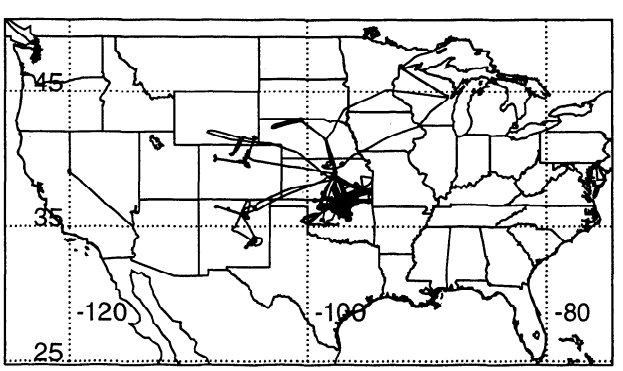

Figure 1. SUCCESS flight tracks out of Salina, Kansas (April 15 - May 8, 1996).

HCN concentration of 200 pptv, this yields an interference of 2-15 pptv due to HCN, which is small compared to observed levels of NO_y in the upper troposphere (300-1000 pptv).

Chemical steady state model calculations of the NO_x/NO_y concentration ratio were made using the Harvard 0-D model constrained with local 1-minute averaged observations of O_3, CO, NO, H_2O, CH_4, pressure, temperature, and aerosol surface area (specified from observed aerosol number concentrations and size distributions). Model calculations were performed for a total of 2770 individual points along the aircraft flight tracks. The model calculates the chemical diel steady state concentrations of 30 species including NO_2, NO_3, N_2O_5, HNO_2, HNO_4, HNO_3, PAN. Total NO_t ($=NO+NO_2+NO_3+2N_2O_5+HNO_2+HNO_4$) is assumed constant over the diel cycle and is calculated iteratively in the model to match the observed NO at the time of day of observations. The reader is referred to *Jaeglé et al.* [this issue] for further discussion of the application of the model to the SUCCESS data.

Origin of NO_y in the Upper Troposphere

Mean observed concentrations of O_3, CO, NO, and NO_y above the central United States are listed in Table 1. Measurements made in fresh aircraft exhaust and in the stratosphere were excluded from the means. Concentrations of NO_x listed in the Table are the sum of observed NO and steady state NO_2 derived from the photochemical model. High concentrations of NO_y and CO below 6 km altitude reflect surface sources from fossil fuel combustion. The secondary maxima for NO, NO_y, and CO in the upper troposphere at 10-12 km result in a C-shaped vertical profile for these species, as observed in previous studies [*Drummond et al.*, 1988; *Ridley et al.*, 1994].

Four sources can contribute to the elevated NO_y concentrations in the upper troposphere: lightning, aircraft, transport from the stratosphere, and convective transport of fossil fuel combustion products from the boundary layer. To distinguish between these possible sources, atmospheric concentrations of NO_y can be related to concurrent measurements of CO, a long-lived tracer of anthropogenic pollution. We use NO_y, instead of NO or NO_x, as a tracer of nitrogen oxides because it is chemically conserved (although it is removed by deposition).

The relationship between observed NO_y and CO in the upper troposphere is shown in Figure 2, which combines all the measurements obtained over the central United States above 8 km during SUCCESS. As in Table 1, observations made in fresh aircraft plumes have been excluded. The data have been separated in four categories to highlight the different origins of NO_y.

Data with CO between 80 and 150 ppbv and NO_y between 100 and 500 pptv represent the bulk of the observations (black dots in Figure 2). These data show a general positive correlation between CO and NO_y (least squares correlation coefficient R>0.7 for almost half of the individual flights). On one occasion, the May 2 flight, values of CO as high as 250 ppbv were observed in the upper troposphere (blue pluses in Figure 2). These high values were correlated with high NO_y. The general correlation of

Table 1. Average concentrations over the central United States.

	Altitude				
	2-4 km	4-6 km	6-8 km	8-10 km	> 10 km
O_3 (ppbv)	52 (7)	61 (8)	60 (24)	60 (14)	70 (15)
CO (ppbv)	146 (18)	155 (65)	126 (28)	108 (15)	132 (38)
NO (pptv)	59 (43)	39 (32)	39 (45)	30 (22)	61 (45)
NO_x (pptv)	104 (103)	53 (25)	50 (60)	49 (48)	70 (51)
NO_y (pptv)	702 (497)	821 (782)	380 (348)	265 (90)	368 (114)

Tropospheric measurements made during SUCCESS (April-May 1996) in flights out of Salina, Kansas (Figure 1). Standard deviations are in parenthesis. Observations made in fresh aircraft exhaust (CO_2>368 ppmv and NO> 300 pptv) and in the stratosphere (O_3>100 ppbv and N_2O<310 ppbv) were excluded from the averages. NO_x = observed NO + model calculated steady state NO_2.

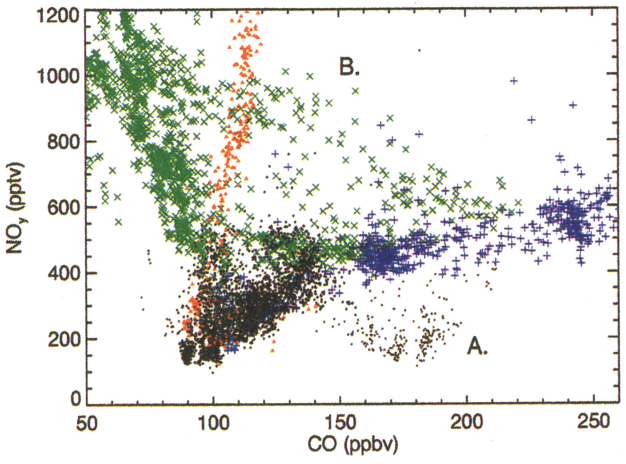

Figure 2. Observed NO_y versus CO concentrations for altitudes between 8 and 12.5 km over the central United States (Figure 1). Each point is a 10-second average. Four populations are highlighted. The green crosses represent stratospheric data (N_2O<310 ppbv and O_3>100 ppbv). The blue pluses represent the flight of May 2 (strong convective influence), and the red triangles represent the flight of May 8 (strong lightning influence). The remaining data (black dots) are viewed as representing the upper tropospheric background. Fresh aircraft plume observations (CO_2>368 ppmv and NO>300 pptv) have been excluded from this figure. Populations "A" and "B" are discussed in the text.

CO with NO_y in the background air indicates that convection of polluted boundary layer air constitutes a strong source of NO_y in the upper troposphere. The NO_x/CO ratio from anthropogenic sources in the United States is ~ 0.1 [*EPA*, 1995], much higher than the observed $\Delta NO_y/\Delta CO$ ~ 0.005 in the upper troposphere in SUCCESS (Figure 2). Loss of NO_y by deposition in the boundary layer could provide an explanation for this. A 3-D model calculation of the NO_y budget over the United States in spring [*Liang et al.*, 1997] indicates that the $\Delta NO_y/\Delta CO$ ratio in convective plumes pumped to the upper troposphere should be only 20% of the NO_y/CO source ratio in the United States, due to loss of HNO_3 by deposition in the boundary layer and in precipitation associated with the convective plumes. In that 3-D model, NO_y injected to the upper troposphere from U.S. pollution is on average 60% NO_x, 30% PAN, and 10% other organic nitrates (the model assumes 100% scavenging of HNO_3 in deep wet convection).

The continental boundary layer origin of air in the upper troposphere during SUCCESS is also supported by observations of aerosol composition [*Talbot et al.*, this issue]. Global 3-D model studies and analyses of cloud top data have previously suggested that deep convection over the central United States is a major export pathway for pollution from North America [*Jacob et al.*, 1993; *Thompson et al.*, 1994].

An anomalous population of points with high CO (150-200 ppbv) and low NO_y (150-250 pptv) can be seen in Figure 2 (population of points labeled by "A"). These observations were made on April 18 when, on a few instances, nitrate in the aerosol phase was as abundant as gas phase NO_y. Partitioning of NO_y between the gas and aerosol phases could account for part of the anomaly.

Observations in the stratosphere, as diagnosed by N_2O<310 ppbv and O_3>100 ppbv, are shown as green crosses in Figure 2. Concentrations of CO and NO_y are in general anticorrelated, as would be expected. However, a significant ensemble of stratospheric data (labeled by "B" in Figure 2) seem to fall along a mixing line between stratospheric air (low CO and high NO_y) and polluted air originating from the boundary layer (high CO and high NO_y). This could be explained by stratosphere-troposphere exchange due to convective clouds overshooting into the lowermost stratosphere [*Poulida et al.*, 1996].

Lightning NO_x was observed on the May 8 flight (red triangles) which sampled the outflow of a mesoscale convective system. Concentrations of NO_y were very high (up to 2 ppbv), and 80% of NO_y was in the form of NO. The relatively low CO concentrations associated with those high levels of NO_y allow to clearly distinguish the lightning source of NO_y from the fossil fuel combustion source.

Outside of fresh exhaust plumes, we could not detect an NO_y signal from aircraft emissions. We searched for such a signal as a correlation of NO_y with CO_2 not associated with CO (since aircraft have low CO/CO_2 emission ratios) but none was apparent. Difficulty arises in this analysis due to variability in the CO_2 background concentrations.

The NO_x/NO_y Ratio

NO_y is supplied to the upper troposphere from primary sources as NO_x (and also, in the case of convective injection of U.S. pollution, as PAN). Subsequent oxidation of NO_x to non-radical reservoirs (HNO_3, HNO_4, PAN), followed by regeneration of NO_x from these reservoirs, represents a chemical cycle for NO_x within the NO_y chemical family which could play an important role in regulating NO_x concentrations in the upper troposphere. We find in our model calculations that the cycling between NO_x and HNO_3 is the most important, as PAN has a long lifetime and HNO_4 concentrations are relatively low.

NO_2 is oxidized to HNO_3 by daytime reaction with OH, or by nighttime formation of N_2O_5 followed by hydrolysis on sulfate aerosols:

$$NO_2 + OH + M \rightarrow HNO_3 + M \quad (1)$$

$$N_2O_5 + H_2O\,(\text{aerosols}) \rightarrow 2\,HNO_3. \quad (2)$$

The lifetime of NO_x against conversion to HNO_3 depends on the NO_2/NO ratio because NO_2 is the reactant species for the conversion. Recycling of NO_x from the HNO_3 reservoir is by photolysis and reaction with OH:

$$HNO_3 + h\nu \rightarrow NO_2 + OH \quad (3)$$

$$HNO_3 + OH \rightarrow NO_3 + H_2O. \quad (4)$$

Figure 3 shows the observed NO_x/NO_y concentration ratios (where NO_x = observed NO + modeled NO_2) in SUCCESS as a function of altitude, and compares them to values obtained in our diel steady state photochemical model calculations along the aircraft flight tracks. The observed NO_x/NO_y ratio is highly variable in the upper troposphere above 8 km, with values ranging from below 0.1 to 0.8 mol/mol, the average being 0.2 mol/mol. The NO_x/NO_y ratios predicted by the steady state model are much less variable (0.05 to 0.15 mol/mol) and are in general 30-60% lower than the observations. In the lower troposphere, below 6 km, better agreement between model and observations is reached by inclusion of HNO_3 rainout in the model with the time constants from *Giorgi and Chameides* [1985]. At high altitude, rainout is much slower and cannot explain the discrepancy.

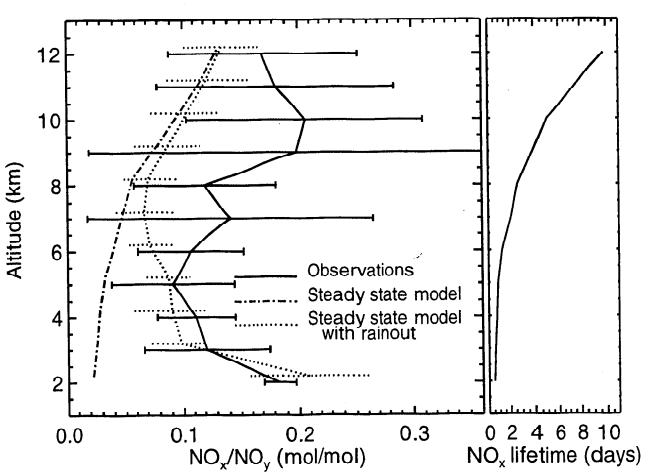

Figure 3. NO_x/NO_y concentrations ratios as a function of altitude over the central United States during SUCCESS (NO_x = observed NO + modeled NO_2). Mean observations (solid line) are compared to results from the steady state 0-D model calculations along the aircraft flight tracks with rainout (dotted line) and without rainout (dash-dotted line). Horizontal bars show standard deviations. The right panel shows the chemical lifetime of NO_x against oxidation to HNO_3 in the 0-D model.

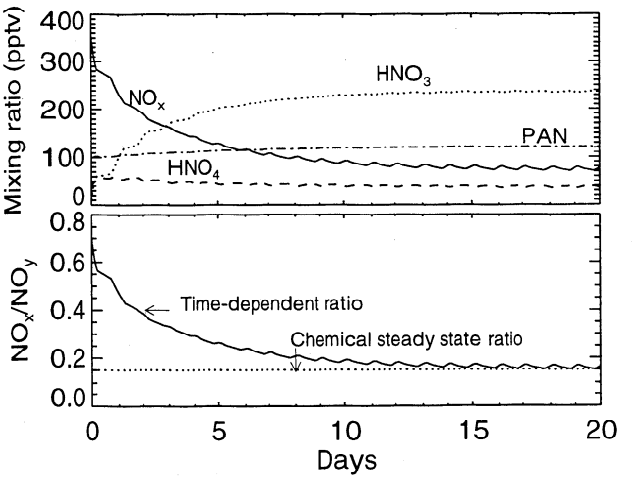

Figure 4. Time-dependent model calculation of the NO_y partitioning following injection of fresh NO and PAN in the upper troposphere. The conditions of the calculation correspond to the average observations at 10-12 km during SUCCESS (Table 1).

Above 8 km, both observed and modeled NO_x/NO_y ratios show a general increase with altitude, reflecting the increasing lifetime of NO_x. Figure 3 (right panel) shows the lifetime of NO_x in the model against conversion to HNO_3, its principal sink. The lifetime increases from 1 day at 3 km to 8 days at 11 km, in large part because of the temperature dependence of the reaction of NO with O_3 and the resulting partitioning of NO_x as NO at the higher altitudes (Table 1). In a companion paper we find that upper tropospheric HO_x observations tend to be underestimated by the steady state model, which we suggest is due to a strong source of HO_x from convective injection of peroxides and formaldehyde produced in the boundary layer [*Jaeglé et al.*, this issue]. When the model is constrained to reproduce the observed OH, the NO_x lifetime is reduced to 6 days at 11 km.

N_2O_5 hydrolysis on aerosols contributes up to 10-30% of NO_x loss. Even if we neglect N_2O_5 hydrolysis (assuming that the aerosols are dry and unreactive) the model still underestimates the observed NO_x/NO_y ratios in the upper troposphere.

Because of the long lifetime of NO_x in the upper troposphere (Figure 3) and the strong source from convection (Figure 2) we need to evaluate the possibility that the partitioning between NO_x and HNO_3 has not reached chemical steady state. To illustrate this point, the evolution of the NO_x/NO_y ratio following a primary injection of NO and PAN in the upper troposphere is shown in Figure 4 for a time dependent model calculation at 11 km. Over a one week time period, NO is converted to HNO_3, and the NO_x/NO_y ratio decreases from 0.6 to 0.2. Four days after the initial injection, the NO_x/NO_y ratio is still twice the chemical steady state value.

Following on this idea, we examined the relationship between the observed NO_x/NO_y ratio and the age of the air in the upper troposphere. Previous studies have used ratios of short-lived hydrocarbons as indicators of the age of the air [*McKeen et al.*, 1995]. In the absence of such hydrocarbon observations during the SUCCESS mission, we use the number concentration of condensation nuclei (CN) (defined as particles with diameters larger than 0.007 μm) as proxy for the age of air in the upper troposphere. Condensation nuclei are generally elevated in air which has undergone recent convection, because of injection of precur-

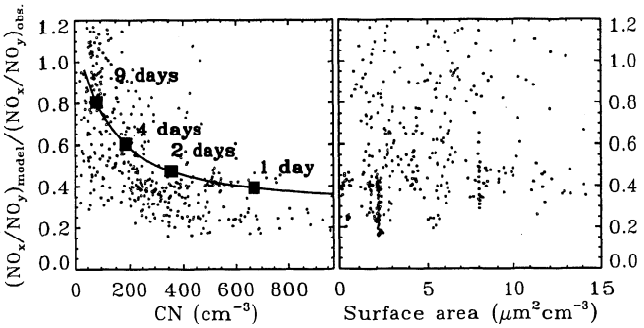

Figure 5. Left panel: Departure of the NO_x/NO_y concentration ratio from chemical steady state (model-calculated steady state NO_x/NO_y divided by the observed NO_x/NO_y) as a function of condensation nuclei (CN) number concentration. The data are from all the SUCCESS flights over the central United States (Figure 1) above 8-km altitude. Observations in clouds (acrosol surface area > 20 $\mu m^2/cm^3$) and aircraft exhaust plumes have been excluded. CN is used as a proxy for the time elapsed since the last convective event. The solid curve shows results from a time-dependent model calculation of the NO_x/NO_y ratio where the time coordinate is derived from the CN concentration (see text). Right panel: Same as left panel, but as a function of aerosol surface area.

sor gases which generate new particles by homogeneous nuclcation. This process is facilitated by the scavenging of big particles on which the precursor gases might have condensed instead of forming new particles [*Clarke*, 1992]. Subsequent coagulation and diffusion to other aerosols decreases the CN number concentration on a time scale of days. While CN concentrations tend to be dominated by ultra fine particles, the total surface area is controlled by the larger particles and the two are generally anticorrelated [*Clarke*, 1992].

Figure 5 (left panel) shows the departure from steady state of the NO_y partitioning – represented by the ratio of modeled NO_x/NO_y to observed NO_x/NO_y – plotted as a function of observed CN concentration for altitudes above 8 km. A general tendency for better agreement at lower CN concentrations (aged air) can be seen in Figure 5, while the agreement is worst for high CN concentrations (fresh air).

We can approximately relate CN concentrations, N(t), to the time elapsed since the last convective event by the following simplified solution to the coagulation equation [*Seinfeld*, 1986]:

$$N(t) = N_o / (1 + t/\tau), \quad (5)$$

where N_o is the initial concentration of CN and τ the coagulation time constant. τ is defined as $\tau = 2/(K \times N_o)$, where K is the Brownian coagulation coefficient of the particles. Assuming N_o = 5000 cm^{-3} and $K = 3.0 \times 10^{-8}$ cm^3 s^{-1} for particles with diameters of 0.01 μm coagulating on a background population of 0.1 μm diameter (based on the observed aerosol size distributions during SUCCESS), we obtain $\tau \sim 4$ hours. The age of the air inferred from this CN proxy is shown in Figure 5, together with the corresponding departure from photochemical equilibrium expected from our previously described time-dependent model calculation. It appears from this calculation that the time required for the NO_x/NO_y ratio to relax to chemical steady state following a fresh injection of NO_x can explain the discrepancy between observations and the steady state model. The variability in the observed NO_x/NO_y ratio (Figure 3) could be explained by the range of chemical ages for the air sampled.

The right panel in Figure 5 shows the same departure from chemical steady state as in the left panel, but plotted as a function of the aerosol surface area measured during SUCCESS. If a fast heterogeneous conversion of HNO_3 to NO_x were occurring, we would expect the largest discrepancy between model and observations of NO_x/NO_y at high surface areas. Better agreement at low surface areas would also be expected. No obvious trend can be seen in the right panel of Figure 5. Thus, our analysis of the SUCCESS observations in the upper troposphere does not provide evidence of heterogeneous recycling of HNO_3 to NO_x.

Acknowledgments. This work was supported by the National Aeronautics and Space Administration (NASA-NAG5-2688). The aerosol surface area measurements were provided by D. Baumgardner from NCAR.

References

Brasseur, G.P., *et al.*, Atmospheric impact of NO_x emissions by subsonic aircraft: a three-dimensional model study, *J. Geophys. Res.*, *101*, 1423-1428, 1996.

Chatfield, R.B., Anomalous HNO_3/NO_x ratio of remote tropospheric air: conversion of nitric acid to formic acid and NO_x?, *Geophys. Res. Lett.*, *21*, 2705-2708, 1994.

Clarke, A.D., Atmospheric nuclei in the remote free-troposphere, *J. Atmos. Chem.*, *14*, 479-488, 1992.

Drummond, J.W., *et al.*, Measurements of nitric oxide between 0-12 km altitude and 67°N to 60°S latitude obtained during STRATOZ III, *J. Geophys. Res.*, *93*, 15,831-15,849, 1988.

Environmental Protection Agency, National air pollution and emission trends 1900-1994, *Ref. EPA-454/R-95-011*, EPA, Research Triangle Park, NC, 1995.

Fan, S.-M., *et al.*, Origin of tropospheric NO_x over subarctic eastern Canada in summer, *J. Geophys. Res.*, *99*, 16,867-16,877, 1994.

Fishman, J. *et al.*, Observational and theoretical evidence in support of a significant in situ photochemical source of tropospheric ozone, *Tellus*, *31*, 432-446, 1979.

Giorgi, F., and W.L. Chameides, The rainout parameterization in a photochemical model, *J. Geophys. Res.*, *90*, 7872-7880, 1985.

Hauglustaine, D.A., *et al.*, HNO_3/NO_x ratio in the remote troposphere during MLOPEX-2: Evidence for nitric acid reduction on carbonaceous aerosols?, *Geophys. Res. Lett.*, *23*, 2609-2612, 1996.

Jacob, D.J., *et al.*, The origin of ozone and NO_x in the tropical troposphere: a photochemical analysis of aircraft observations over the South Atlantic Basin, *J. Geophys. Res.*, *101*, 24,235-24,250, 1996.

Jacob, D.J., *et al.*, Factors regulating ozone over the United States and its export to the global atmosphere, *J. Geophys. Res.*, *98*, 14,817-14,826, 1993.

Jaeglé, L., *et al.*, Sources of HO_x and production of ozone in the upper troposphere over the United States, *Geophys. Res. Lett.*, this issue.

Kliner, D., et al., Laboratory investigation of the catalytic reduction technique for measurement of atmospheric NO_y, *J. Geophys. Res.*, *102*, 10,759-10,779, 1997.

Lacis, A.A., *et al.*, Radiative forcing of climate by changes in the vertical distribution of ozone, *J. Geophys. Res.*, *95*, 9971-9981, 1990.

Liang, J., *et al.*, Seasonal budgets of reactive nitrogen species and ozone over the United States, and export fluxes to the global atmosphere, *J. Geophys. Res.*, *in press*, 1997.

Liu, S.C., et al., A study of the photochemistry and ozone budget during the Mauna Loa Observatory Photochemistry Experiment, *J. Geophys. Res*, *97*, 10463-10471, 1992.

McKeen, S.T., *et al.*, Hydrocarbon ratios and photochemical history of air masses, *Geophys. Res. Lett.*, *20*, 2363-2366, 1995.

Poulida, O., *et al.*, Stratosphere-troposphere exchange in a mid-latitude mesocale convective complex. 1. Observations, *J. Geophys. Res.*, *101*, 6823-6836, 1996.

Ridley, B.A., *et al.*, Distribution of NO, NO_x, NO_y, and O_3 to 12 km altitude during the summer monsoon season over New Mexico, *J. Geophys. Res.*, *99*, 25,519-25,534, 1994.

Scinfeld, J.H., Atmospheric chemistry and physics of air pollution, *edited by Wiley & sons*, 1986.

Talbot, R.W., *et al.*, Influence of vertical transport on free tropospheric aerosols over the central USA in springtime, *Geophys. Res. Lett.*, this issue.

Thompson, A.M., *et al.*, Convective transport over the central United States and its role in regional CO and ozone budgets, *J. Geophys. Res.*, *99*, 18,703-18,711, 1994.

Toon, O.B., *et al.*, Overview of SUCCESS, *Geophys. Res. Lett.*, this issue.

T.L. Campos, B.A. Ridley, A.J. Weinheimer, Atmospheric Chemistry Division, NCAR, Boulder, CO 80307.

D.E. Hagen, Department of Physics, University of Missouri, Rolla, MO 65401.

D.J. Jacob, L. Jaeglé (corresponding author), and Y. Wang, Department of Earth and Planetary Sciences, Harvard University, 29 Oxford Street, Pierce Hall, Cambridge, MA 02138. (e-mail:lyj@io.harvard.edu)

G.W. Sachse, NASA Langley Research Center, Hampton, VA 23681.

(Received July 17, 1997; revised October 22, 1997;
accepted: October 27, 1997)